Optics Letters

High-average-power single-frequency pulse optical parametric oscillator based on pulse-integrated seed-injection automatic locking

Jiaqi Song,[1] Jiliang Qin,[1,2] Xuechen Cao,[1] Donglin Cheng,[1] Yanan Chen,[1] and Huadong Lu[1,2,*]

[1]State Key Laboratory of Quantum Optics and Quantum Optics Devices, Institute of Opto-Electronics, Shanxi University, Taiyuan 030006, China
[2]Collaborative Innovation Center of Extreme Optics, Shanxi University, Taiyuan 030006, China
*luhuadong@sxu.edu.cn

Received 20 February 2024; revised 18 March 2024; accepted 25 March 2024; posted 26 March 2024; published 24 April 2024

Near-infrared nanosecond (ns) single-longitudinal-mode (SLM) pulse light generated from an optical parametric oscillator (OPO) is an important source in nonlinear optics and high-precision spectral analysis. In this Letter, a stable SLM near-infrared ns pulse light source generated from the OPO is presented, which is achieved by developing a seed-injection automatic locking technique based on a pulse-integrated photodetector (PIPD). Depending on the PIPD, the peak power of the pulse light detected by the photodiode is converted to the average power by integrating several pulses. As a result, the detector saturation is thoroughly eliminated, and the interference signal including the resonance point between seed and pulse lights can easily be attained by scanning the resonator length. On this basis, a microcontroller unit (MCU) is employed to realize automatic locking by looking for the minimum value of the interference signal. Finally, a SLM 824 nm pulse light source with an output power of 20.5 W and a linewidth of 51.42 MHz is obtained. The presented method can pave the way to implement a low-cost and compact high-average-power SLM pulse OPO. © 2024 Optica Publishing Group

https://doi.org/10.1364/OL.521977

Near-infrared nanosecond (ns) single-longitudinal-mode (SLM) pulse light source generated from the optical parametric oscillator (OPO) has been applied in lots of science and technology fields including nonlinear optics [1], time-resolved spectroscopy [2], laser resonance ionization spectroscopy [3], and differential absorption lidar [4] owing to its intrinsic advantages of high output power, good beam quality, and wide output spectrum. The SLM pulse OPOs can be achieved by employing mode-selection elements including an etalon and a volume Bragg grating cavity mirror, but the output power is easily restricted by the loss of these mode selectors and their damage threshold. On the contrary, the seed-injection locking is a good candidate to achieve a SLM pulse OPO with free of loss. To lock the resonator of the OPO to the oscillating frequency of the seed laser, it is necessary to discriminate the difference between the oscillating frequency and that of the seed laser and then dynamically adjust the cavity length through the negative feedback control system according to the obtained error signal. In order for this purpose to be realized, the Hansch–Couillaud (HC) locking technique based on the laser polarization and the Pound–Drever–Hall (PDH) technique based on the phase modulation are developed and become more and more popular. However, for a SLM pulse OPO based on the seed-injection locking, the influence of the generated pulse light on the locking effect of the seed laser has to be considered because the peak power of the pulse light is often far higher than the power of the seed laser. In 2017, Sonnenschein *et al.* developed a detector based on a synchronous switch, which was deactivated during the presence of the pulse laser and activated when only a seed laser is present [5]. Although the signal-to-noise ratio (SNR) of the error signal is greatly improved because of the absence of the pulse laser, the switching process introduced additional noise to the error signal. Recently, our group has developed a pulse saturation seed-injection locking method based on the PDH technique, and the disturbance of the pulse light on the locking of the injected seed laser has successfully eliminated [6]. However, too many components, including optical and electronic parts, increased its complexity. In 2021, Wei *et al.* reported an intracavity seed-injection technique which was implemented by a hybrid OPO architecture combining pulse and continuous wave (CW) operation in a single optical cavity using two identical nonlinear crystals [7]. In 2022, Sonnenschein *et al.* achieved a self-seeded hybrid CW and pulsed Ti:sapphire laser system in a single optical cavity. The precise and mode-hop-free control of the laser frequency was realized by tuning the dither frequency to maximize the error signal [8]. In the same year, Granados *et al.* demonstrated a direct and simple route for the generation of SLM light relying on phonon-resonant Raman interactions within a monolithic diamond resonator. This technique did not require elaborate mechanical feedback loops [9]. However, these methods have high requirements for cavity design. Therefore, employing a SLM CW laser as the seed laser for attaining a SLM pulse OPO is still the most popular candidate so far. Factually, when a SLM CW laser as a seed laser is injected into a high-average-power pulse OPO, the seed laser reflected

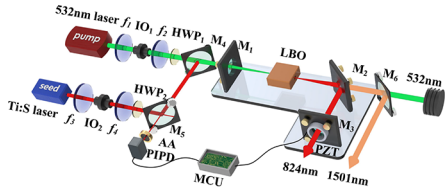


Fig. 1. Schematic diagram of the seed-injection locking OPO.

from the cavity mirror and the generated pulse light leaked from the cavity mirror will destruct the interference with each other when their frequencies are the same. In other words, once the length of the cavity is scanned, a periodic interference signal is generated, and the minimum value represents the resonance point between the seed and pulse lights. However, compared with the pulse light with high peak power, the obtained interference signal is so small that it is easily submerged by the pulse noise. At the same time, the adopted photodetector (PD) is easily saturated by the high peak power of the pulse light. As a result, it is difficult to obtain an effective high SNR locking signal in a high-average-power pulse OPO. To address this issue, in this Letter, we report a seed-injection automatic locking technology based on the principle of destructive interference. By designing a pulse-integrated photodetector (PIPD) for improving the SNR of the interference signal and employing a microcontroller unit (MCU) to realize automatic locking by looking for the minimum value of the interference signal, the built OPO is successfully locked to the injected seed laser, and a SLM 824 nm pulse light with an average output power of 20.5 W and a linewidth of 51.42 MHz is finally achieved.

The experimental schematic of the designed seed-injection automatic locking OPO is depicted in Fig. 1, where the optical structure of the OPO is the same as that presented in Ref. [6]. The free spectral range (FSR) and the quality factor of the OPO are 770 MHz and 1.54×10^7, respectively. A homemade pulse 532 nm laser with a repetition frequency and a pulse width of 50 kHz and 13 ns, respectively, acts as the pump source. The output 532 nm laser beam is shaped and focused by lenses f_1 and f_2 and then firstly injected into the OPO resonator consisting of M_1, M_2, and M_3 to pump the LBO crystal. M_1 is coated with a high-reflection (HR) film at 824 nm ($R = 99.5\%$) and a high-transmission (HT) film at 532 nm, while M_2 is coated with the HR film at 824 nm and the HT film at 532 and 1501 nm. The output coupling mirror M_3 is coated with a partially reflective film at 824 nm ($T = 20\%$) and adhered to the piezoelectric transducer (PZT, HPSt 500/10-5/7, piezosystem jena) with a range and a resonant frequency of 7 μm and 40 kHz, respectively. At the same time, the seed laser output from the homemade Ti:sapphire laser with the linewidth of 325 kHz is shaped and focused by lenses f_3 and f_4 and then coupled into the resonator of OPO. When the main part of the generated pulse light is transmitted from M_3, a small part of pulse light can also leak from M_1, which is reflected by M_4 together with the seed laser reflected by the resonator and then detected by the PIPD. To prevent premature saturation of the photodiode, an adjustable attenuator (AA) is installed in front of the PIPD to control the power of the injected light. When only the pump light is injected into the OPO, countless pairs of signal and idler lights can be generated according to the principle of the OPO. Although the resonator can effectively filter sideband modes, lots of modes can still oscillate simultaneously in the resonator. Assuming the mode number is $2m + 1$, the optical field of the

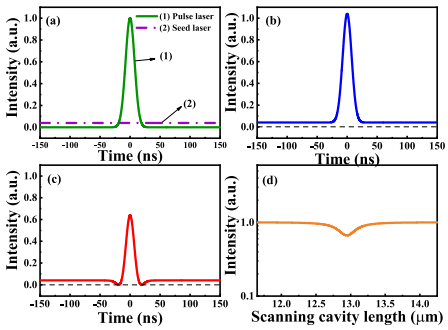


Fig. 2. Theoretical calculation diagram. (a) Light intensity. Detected optical field (b) without interference and (c) with interference. (d) Interference signal.

generated pulse light leaked from M_1 can be expressed as

$$\vec{E}_{c1}(t) = \sqrt{\frac{T_1}{T_3}} \sum_{k=-m}^{m} A_k(t) e^{i(\omega_k t + \psi_k)} e^{-(\frac{t}{\tau})^2}, \tag{1}$$

where $A_k(t)$, ψ_k are the amplitude and the phase of the pulse light with frequency ω_k (k=-m, *ldots*,0, *ldots*m), respectively, $\omega_k = ck/2nL$. T_1 and T_3 are the transmittance of M_1 and M_3, respectively. τ is the pulse width of the pulse light, and L is the length of the OPO cavity. Once the seed laser is injected into the resonator, the optical field of the seed laser reflected by M_1 is

$$\vec{E}_s = \sqrt{H} A_s e^{-i(\omega_0 t + \phi_0)}, \tag{2}$$

$$H = \frac{R_1 + R_3 - 2\sqrt{R_1 R_3} cos(4\pi \Delta L \omega_0 / c)}{1 + R_1 R_3 + 2\sqrt{R_1 R_3} cos(4\pi \Delta L \omega_0 / c)}$$

where A_s, ϕ_0 are the amplitude and the phase of the seed laser with frequency ω_0, respectively. H is the reflection coefficient of the seed laser, and R_1 and R_3 are the reflectance of the M_1 and M_3 of the OPO, respectively, ΔL is the variation in the length of the scanning cavity. The intensity distributions of these two light fields are shown in Fig. 2(a), where the pulse width of the generated pulse light and the center frequency of the seed laser are assumed as $\tau = 15$ ns and $\omega_0 = 3.64 \times 10^{14}$ Hz, respectively. When the resonant frequency of the pulse light is different from that of the seed laser, the OPO resonator outputs a broadband-spectrum light, and no interaction between the two optical fields occurs. The light intensity of the detected optical field is

$$I_1(t) = |\vec{E}_{c1}(t)|^2 + |\vec{E}_s|^2 = \frac{T_1}{T_3} \sum_{k=-m}^{m} {A_k}^2(t) e^{-2(\frac{t}{\tau})^2} + H A_s^2. \tag{3}$$

The light intensity of the detected optical field is the power sum of the seed laser and the pulse light, which is illustrated in Fig. 2(b), where the dashed line represents zero light intensity. However, when the pulse light will work with the same frequency ω_0 of the seed laser due to the frequency pulling of the seed laser, the sideband modes of the OPO can be effectively suppressed, and the optical field of the pulse light can be expressed as

$$\vec{E}_{c2}(t) = \sqrt{T_1/T_3} A_c(t) e^{i(\omega_0 t + \psi_0)} e^{-(\frac{t}{\tau})^2}, \tag{4}$$

where $A_c(t)$, ψ_0 are the amplitude and the phase of the OPO cavity mode after seed laser injection, respectively. At the same

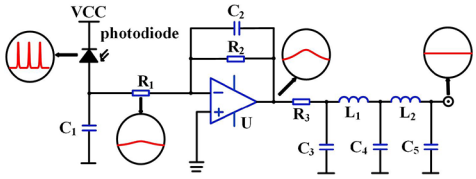


Fig. 3. Schematic diagram of the PIPD.

time, the light intensity of the detected optical field is given by

$$I_2(t) = |\vec{E}_{c2}(t)|^2 + |\vec{E}_s|^2 - 2\vec{E}_{c2}(t)\vec{E}_s = (T_1/T_3)A_c{}^2(t)\, e^{-2(\frac{t}{\tau})^2} + HA_s{}^2 - 2\sqrt{HT_1/T_3}A_sA_c(t)e^{-(\frac{t}{\tau})^2}, \quad (5)$$

where the phase difference of $(2n + 1)\pi$ between the leaked pulse light and the reflected seed laser has been added. The corresponding intensity distribution diagram is depicted in Fig. 2(c), which reveals that most of the seed laser will enter the OPO cavity and subsequently leaked from M_3 along with the generated pulse light when the seed light resonates with the OPO cavity. In other words, the total intensity of the light leaked from M_1 is obviously decreased. In order to make the average power of the pulse light and the power of the seed laser basically on the same order of magnitude, the peak power of the pulse light is converted into an average power by integrating multiple pulses in a period of time. In this case, once the length of the OPO is scanned, the interference signal shown in Fig. 2(d) can be obtained. However, when a common detector is used to detect the light field, the interference signal is too small to be easily overwhelmed owing to the high peak power of the pulse light. Moreover, in this process, the high peak power of the pulse signal also easily saturated the detector and resulted in a failure to attain the interference signal. To address this issue, a novel PIPD containing a photodiode, a RC circuit, a transimpedance amplifier, and a five-order low-pass filter is designed, as shown in Fig. 3. The photodiode (s3399, Hamamatsu) converts the pulse light signal into a current signal, and the resulting charges accumulate in capacitor 1 (C_1 = 150 nF). C_1 and resistance 1 (R_1 = 2 kΩ) make up the RC circuit, where R_1 is further used to control the rate of the charge accumulation and limited the bandwidth of current accumulation. The bandwidth of the RC circuit is about 530 Hz, which ensured the unsaturated and responsive PIPD. Then the current output from R_1 is converted into a voltage signal by a transimpedance amplifier consisting of C_2 (C_2 = 300 nF), R_2 (R_2 = 10 kΩ), and U (OPA1656). The −3 dB bandwidth of the transimpedance amplifier is 70 Hz, which enables the PIPD to achieve a high SNR. Even so, there is still a large signal fluctuation at the high-frequency range because of the high peak power for the pulse light with the repetition rate of 50 kHz. Therefore, the five-order low-pass filter with a cutoff frequency of 4.8 kHz is used to reduce the high-frequency noise. Herein, $C_3 = C_5 = 4.7$ μF, $C_4 = 14$ μF, $R_3 = 10$ Ω, and inductances $L_1 = L_2 = 330$ μH.

Figure 4 depicts the attained interference signals for the common detector and the PIPD, respectively. When the power of the injected seed laser and the output pulse light are 200 mW and 20 W, respectively, it is difficult for a common detector to obtain an effective interference signal due to the influence of the pulse light with high peak power, as shown in Fig. 4(a), where the amplitudes of the interference signal detected by the common detector and the standard deviation (SD) of the noise are 0.18 V and 0.066 V, respectively, and then the SNR of the interference

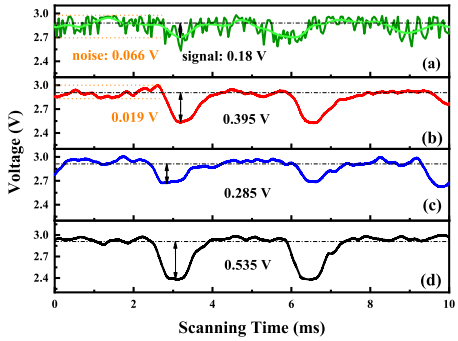


Fig. 4. Interference signals with different conditions. (a) Common PD and (b) PIPD, 200 mW seed laser and 20 W pulse light. (c) PIPD, 100 mW seed laser and 20 W pulse light. (d) PIPD, 200 mW seed laser and 10 W pulse light.

signal for the common PD is only 4.36 dB. Once the common detector is replaced by the designed PIPD, the clear interference signal is obtained, as shown in Fig. 4(b), where the dash line indicates the average value of the signal in the non-resonance. The amplitude of the interference signal is increased to 0.395 V and the SD of the noise is decreased to 0.019 V. In this case, the achieved SNR of the interference signal for the PIPD in Fig. 4(b) is 13.2 dB, which is higher than that for the common PD which is 4.36 dB. The results demonstrate that the PIPD exhibits superior capability to eliminate the impact of the pulse light compared to a common detector and the interference signal with higher SNR can be obtained. In order to further study the influence of the power difference between the seed laser and the pulse light on the SNR of the interference signal, the power of injected seed light is reduced to 100 mW, while the pulse light power is a constant, the amplitude of the interference signal is 0.285 V, as shown in Fig. 4(c). Conversely, when the power of the seed light remains unchanged, and the power of the output pulse light is reduced to 10 W, the amplitude of the interference signal is 0.535 V, as shown in Fig. 4(d). It is clear from the results that the smaller the average power difference between the seed laser and the pulse light, the higher the SNR of the interference signal.

After obtaining the interference signal with high SNR by the developed PIPD, a MCU-based (ADuC7020, Analog Devices, Inc.) locking system is employed to automatically lock the OPO cavity to the seed laser. As depicted in Fig. 5, the interference signal acquired by the PIPD is used as the input signal and transmitted to the MCU via the analog-to-digital conversion (ADC). There are two operation modes in the MCU-based locking system, which are termed scanning mode and locking mode, respectively. In the scanning mode, the MCU generates a triangular wave signal presented as curve (1) in Fig. 6(a), which acted as the scanning signal. When only the pump laser is injected into the OPO cavity and the seed laser is non-resonate

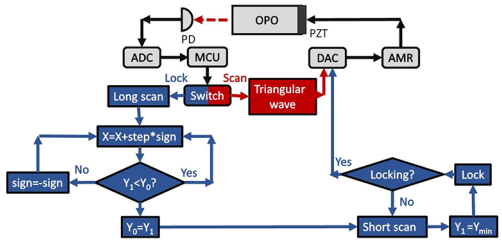


Fig. 5. MCU-based automatic locking program.

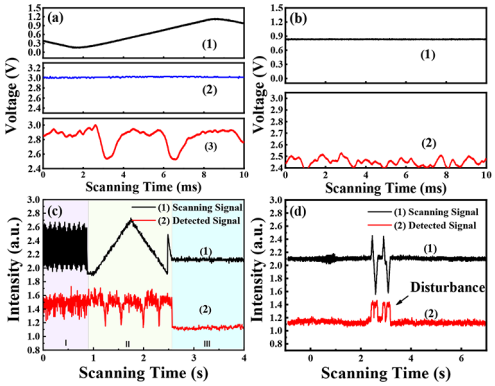


Fig. 6. (a) Scanning signal and detected signal under the scanning state. (b) Scanning signal and detected signal under locking state. (c) Automatic locking process: region I, scanning process; region II, searching the minimum value after switching to the locking mode; region III, implementing the lock. (d) Automatically recover from disturbance.

with the OPO, the signal measured by the PIPD is the power sum of the seed light reflected by M_1 and the pulse light leaked from M_1, as curve (2) in Fig. 6(a). Once the seed and pump lasers are simultaneously injected into the OPO, an obvious interference signal depicted as curve (3) in Fig. 6(a) is obtained. The highest and lowest points of curve (3) coincide with curve (2) in Fig. 6(a) and curve (2) in Fig. 6(b), respectively. When the MCU is switched to the locking mode, a minimum search algorithm [10] within the MCU begins to function, and the process is shown in Fig. 5. After conducting a long scan of the entire cavity length, the minimum value range is initially determined. Subsequently, a short scan is performed within this range to precisely identify the minimum value. The scanning voltage and the detected signal after locking are shown as curves (1) and (2) in Fig. 6(b), respectively. All signals processed by the MCU are transmitted to the PZT through a digital-to-analog conversion (DAC) to control the cavity length of the OPO. The process of automatic locking is explicitly shown in Fig. 6(c). During the locking process, the signal acquired by the PIPD is continuously sampled and compared to its previous measurement to ensure that the system keeps locking at the lowest point of the interference signal throughout. When the system is unlocked due to environmental disturbance, the MCU can promptly recover the lock within 0.3 s. The closed-loop bandwidth of the feedback loop is about 1 kHz. The fastest perturbation that can compensate is about hundreds of hertz. This process is shown in Fig. 6(d).

The linewidth of the pulse light is accurately measured by the beat frequency technique, and the full width at half maximum (FWHM) linewidth obtained is 51.42 MHz, which is shown in Fig. 7(a). On this basis, the maximum output power of the signal and idler lights are 20.5 and 8.15 W at the incident pump power of 48.3 W, respectively, as shown in Fig. 7(b). The overall optical conversion efficiency of the signal and idler lights is remarkably as high as 59.3%. The long-term power stability measured by a powermeter (S425C-L, Thorlabs) is ±1.6% in 1.7 h, and although the power stability is slightly less stable, the system demonstrates good robustness and excellent anti-disturbance ability. The measured pulse width of the output pulse light is 13 ns (inset of Fig. 7(c)). Lastly, the frequency stability is measured by a wavelength meter (WS-6, HighFinesse). The frequency drift of the seed and pulse lights are ±35 and ±55 MHz, respectively, within 1 min, which are depicted in Fig. 7(d).

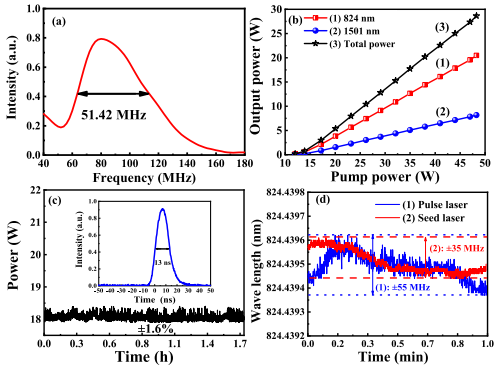


Fig. 7. (a) Linewidth. (b) Output power. (c) Power stability and pulse width. (d) Frequency stability of the 824 nm light.

In conclusion, we present a high-average-power SLM pulse OPO based on pulse-integrated seed-injection automatic locking. A novel PIPD capable of integrating the pulse signal and obtaining the high SNR interference signal is designed by exploiting the destructive interference phenomenon that occurs between the leaked pulse light and the reflected seed laser from the cavity mirror. On this basis, automatic locking has been achieved by using a MCU with a minimal search algorithm, which does not require any modulation or external error signal. As a result, the stable pulse 824 nm OPO with the output power and the linewidth of 20.5 W and 51.42 MHz, respectively, is successfully attained. The seed-injection automatic locking technique based on the pulse-integrated detector presents a novel approach to realize a practical high-average-power SLM pulse OPO.

Funding. National Natural Science Foundation of China (62027821); National Key Research and Development Program of China (2022YFC 2204003); The first Lab-National Innovation Center (Shanxi) science and technology innovation project; Fund for Shanxi "1331 Project" Key Subjects Construction; Research Project Supported by Shanxi Scholarship Council of China (2022-015); Applied Basic Research Project of Shanxi Province (202103021221004); Program for the Innovative Talents of High Education Institution of Shanxi; Special fund for Science and Technology Innovation Teams of Shanxi Province (202204051002005); Applied Basic Research Project of Shanxi Province (202203021212481); Shanxi Province Patent Conversion Project (202305007).

Disclosures. The authors declare no conflicts of interest.

Data availability. Data underlying the results presented in this paper are not publicly available at this time but may be obtained from the authors upon reasonable request.

REFERENCES

1. D. J. Armstrong and A. V. Smith, IEEE J. Sel. Top. Quantum Electron. **13**, 721 (2007).
2. R. Klieber and D. Suter, Phys. Rev. B **73**, 094408 (2006).
3. W. L. Wang, Z. M. Li, X. P. Shen, *et al.*, Spectrosc. Spectral Anal. **37**, 3653 (2017).
4. T. F. Refaat, S. Ismail, A. R. Nehrir, *et al.*, Opt. Express **21**, 30415 (2013).
5. V. Sonnenschein, I. Moore, S. Raeder, *et al.*, Laser Phys. **27**, 085701 (2017).
6. J. L. Qin, J. Q. Song, X. C. Cao, *et al.*, Opt. Lett. **48**, 4973 (2023).
7. J. X. Wei, S. C. Kumar, and M. Ebrahim-Zadeh, Opt. Lett. **46**, 4502 (2021).
8. V. Sonnenschein and H. Tomita, Appl. Sci. **12**, 4727 (2022).
9. E. Granados, C. Granados, R. Ahmed, *et al.*, Optica **9**, 317 (2022).
10. K. Huang, H. Le Jeannic, J. Ruaudel, *et al.*, Rev. Sci. Instrum. **85**, 123112 (2014).